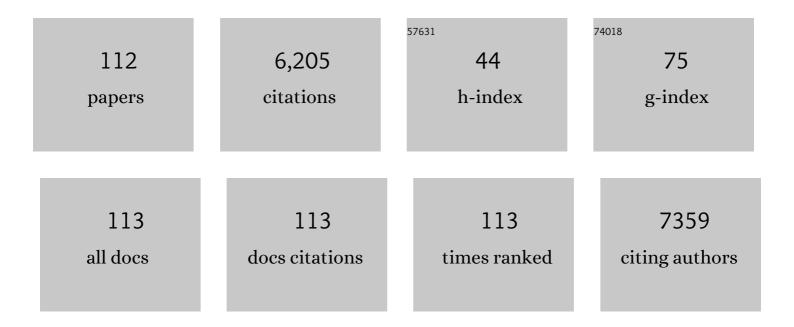
List of Publications by Year in descending order

Source: https://exaly.com/author-pdf/3108102/publications.pdf Version: 2024-02-01



VIINEEL RU

#	Article	IF	CITATIONS
1	Aminoâ€Assisted Anchoring of CsPbBr <sub>3</sub> Perovskite Quantum Dots on Porous g <sub>3</sub> N <sub>4</sub> for Enhanced Photocatalytic CO <sub>2</sub> Reduction. Angewandte Chemie - International Edition, 2018, 57, 13570-13574.	7.2	432
2	Three-dimensional ultrathin Ni(OH)2 nanosheets grown on nickel foam for high-performance supercapacitors. Nano Energy, 2015, 11, 154-161.	8.2	379
3	A Perovskite Nanorod as Bifunctional Electrocatalyst for Overall Water Splitting. Advanced Energy Materials, 2017, 7, 1602122.	10.2	369
4	Building and identifying highly active oxygenated groups in carbon materials for oxygen reduction to H2O2. Nature Communications, 2020, 11, 2209.	5.8	281
5	A Highly Efficient and Robust Cation Ordered Perovskite Oxide as a Bifunctional Catalyst for Rechargeable Zinc-Air Batteries. ACS Nano, 2017, 11, 11594-11601.	7.3	219
6	Aminoâ€Assisted Anchoring of CsPbBr <sub>3</sub> Perovskite Quantum Dots on Porous g <sub>3</sub> N <sub>4</sub> for Enhanced Photocatalytic CO <sub>2</sub> Reduction. Angewandte Chemie, 2018, 130, 13758-13762.	1.6	172
7	Crystallinity Dependence of Ruthenium Nanocatalyst toward Hydrogen Evolution Reaction. ACS Catalysis, 2018, 8, 5714-5720.	5.5	162
8	Fabrication of 3D Co-doped Ni-based MOF hierarchical micro-flowers as a high-performance electrode material for supercapacitors. Applied Surface Science, 2019, 483, 1158-1165.	3.1	156
9	Enhanced electrochemical properties of a LiNiO <sub>2</sub> -based cathode material by removing lithium residues with (NH <sub>4</sub> ) <sub>2</sub> HPO <sub>4</sub> . Journal of Materials Chemistry A, 2014, 2, 11691-11696.	5.2	135
10	Rational construction of triangle-like nickel-cobalt bimetallic metal-organic framework nanosheets arrays as battery-type electrodes for hybrid supercapacitors. Journal of Colloid and Interface Science, 2019, 555, 42-52.	5.0	131
11	Balancing hydrogen adsorption/desorption by orbital modulation for efficient hydrogen evolution catalysis. Nature Communications, 2019, 10, 4060.	5.8	131
12	Promotional effect of F-doped V2O5–WO3/TiO2 catalyst for NH3-SCR of NO at low-temperature. Applied Catalysis A: General, 2012, 435-436, 156-162.	2.2	125
13	Amino-Assisted NH <sub>2</sub> -UiO-66 Anchored on Porous g-C <sub>3</sub> N <sub>4</sub> for Enhanced Visible-Light-Driven CO <sub>2</sub> Reduction. ACS Applied Materials & Interfaces, 2019, 11, 30673-30681.	4.0	116
14	Highly-efficient visible-light-driven photocatalytic H2 evolution integrated with microplastic degradation over MXene/ZnxCd1-xS photocatalyst. Journal of Colloid and Interface Science, 2022, 605, 311-319.	5.0	112
15	A Highly Efficient and Robust Nanofiber Cathode for Solid Oxide Fuel Cells. Advanced Energy Materials, 2017, 7, 1601890.	10.2	109
16	Synergistic interaction of perovskite oxides and N-doped graphene in versatile electrocatalyst. Journal of Materials Chemistry A, 2019, 7, 2048-2054.	5.2	104
17	Carbonâ€Based Electrocatalysts for Efficient Hydrogen Peroxide Production. Advanced Materials, 2021, 33, e2103266.	11.1	104
18	A durable, high-performance hollow-nanofiber cathode for intermediate-temperature fuel cells. Nano Energy, 2016, 26, 90-99.	8.2	93

#	Article	IF	CITATIONS
19	A Tailored Bifunctional Electrocatalyst: Boosting Oxygen Reduction/Evolution Catalysis via Electron Transfer Between Nâ€Đoped Graphene and Perovskite Oxides. Small, 2018, 14, e1802767.	5.2	85
20	Porous Cobalt Phosphide Polyhedrons with Iron Doping as an Efficient Bifunctional Electrocatalyst. Small, 2017, 13, 1701167.	5.2	82
21	Focus on the modified CexZr1â^'xO2 with the rigid benzene-muti-carboxylate ligands and its catalysis in oxidation of NO. Applied Catalysis B: Environmental, 2014, 158-159, 258-268.	10.8	80
22	Identifying the structure of Zn-N2 active sites and structural activation. Nature Communications, 2019, 10, 2623.	5.8	79
23	Electrospun Porous Perovskite La <sub>0.6</sub> Sr <sub>0.4</sub> Co <sub>1</sub> <sub>–</sub> <i><sub>x</sub></i> Fe <i><sub>xNanofibers for Efficient Oxygen Evolution Reaction. Advanced Materials Interfaces, 2017, 4, 1700146.</sub></i>	>1@ <sul< td=""><td>o&gt;<b>37₄/sub</b>&gt;<si< td=""></si<></td></sul<>	o> <b>37₄/sub</b> > <si< td=""></si<>
24	In-situ conversion of rGO/Ni2P composite from GO/Ni-MOF precursor with enhanced electrochemical property. Applied Surface Science, 2018, 439, 413-419.	3.1	71
25	Construction of Porous Mo <sub>3</sub> P/Mo Nanobelts as Catalysts for Efficient Water Splitting. Angewandte Chemie - International Edition, 2018, 57, 14139-14143.	7.2	70
26	Revealing Isolated Mâ^'N <sub>3</sub> C <sub>1</sub> Active Sites for Efficient Collaborative Oxygen Reduction Catalysis. Angewandte Chemie - International Edition, 2020, 59, 23678-23683.	7.2	64
27	Controllable synthesis of Ni-Co nanosheets covered hollow box via altering the concentration of nitrate for high performance supercapacitor. Electrochimica Acta, 2016, 215, 500-505.	2.6	63
28	Construction of Porous Mo <sub>3</sub> P/Mo Nanobelts as Catalysts for Efficient Water Splitting. Angewandte Chemie, 2018, 130, 14335-14339.	1.6	58
29	In Site Growth of Crosslinked Nickel–Cobalt Hydroxides@Carbon Nanotubes Composite for a Highâ€Performance Hybrid Supercapacitor. Advanced Materials Interfaces, 2018, 5, 1800438.	1.9	56
30	Aluminum and Nitrogen Codoped Graphene: Highly Active and Durable Electrocatalyst for Oxygen Reduction Reaction. ACS Catalysis, 2019, 9, 610-619.	5.5	56
31	Co,N-codoped graphene as efficient electrocatalyst for hydrogen evolution reaction: Insight into the active centre. Journal of Power Sources, 2017, 363, 260-268.	4.0	55
32	The characterization of CrCe-doped on TiO2-pillared clay nanocomposites for NO oxidation and the promotion effect of CeOx. Applied Surface Science, 2013, 268, 535-540.	3.1	54
33	In Situ Probing of the Mechanisms of Coking Resistance on Catalyst-Modified Anodes for Solid Oxide Fuel Cells. Chemistry of Materials, 2015, 27, 822-828.	3.2	54
34	A highly efficient composite cathode for proton-conducting solid oxide fuel cells. Journal of Power Sources, 2020, 451, 227812.	4.0	54
35	Binary-dopant promoted lattice oxygen participation in OER on cobaltate electrocatalyst. Chemical Engineering Journal, 2021, 417, 129324.	6.6	51
36	Selective catalytic oxidation of NO with O2 over Ce-doped MnOx/TiO2 catalysts. Journal of Natural Gas Chemistry, 2012, 21, 17-24.	1.8	50

#	Article	IF	CITATIONS
37	A Highly Efficient Composite Catalyst Constructed From NH2-MIL-125(Ti) and Reduced Graphene Oxide for CO2 Photoreduction. Frontiers in Chemistry, 2019, 7, 789.	1.8	50
38	Supramolecular Synthesis of Multifunctional Holey Carbon Nitride Nanosheet with Highâ€Efficiency Photocatalytic Performance. Advanced Optical Materials, 2017, 5, 1700536.	3.6	49
39	Redox stability and sulfur resistance of Sm0.9Sr0.1CrxFe1â^'xO3â^'î´ perovskite materials. Journal of Alloys and Compounds, 2013, 578, 60-66.	2.8	48
40	In Situ Fabrication of 3D Octahedral g <sub>3</sub> N <sub>4</sub> /BiFeWO <sub><i>x</i></sub> Doubleâ€Heterojunction for Highly Selective CO <sub>2</sub> Photoreduction to CO Under Visible Light. ChemCatChem, 2018, 10, 4578-4585.	1.8	48
41	Exploration of Co-Fe alloy precipitation and electrochemical behavior hysteresis using Lanthanum and Cobalt co-substituted SrFeO3-δSOFC anode. Electrochimica Acta, 2018, 277, 226-234.	2.6	47
42	Controllable fabrication of uniform ruthenium phosphide nanocrystals for the hydrogen evolution reaction. Chemical Communications, 2019, 55, 7828-7831.	2.2	47
43	Structure–activity relationship of Cr/Ti-PILC catalysts using a pre-modification method for NO oxidation and their surface species study. Physical Chemistry Chemical Physics, 2015, 17, 15036-15045.	1.3	46
44	<i>In situ</i> self-assembly of zirconium metal–organic frameworks onto ultrathin carbon nitride for enhanced visible light-driven conversion of CO <sub>2</sub> to CO. Journal of Materials Chemistry A, 2020, 8, 6034-6040.	5.2	45
45	Effect of nitrogen doping on oxygen vacancies of titanium dioxide supported vanadium pentoxide for ammonia-SCR reaction at low temperature. Journal of Colloid and Interface Science, 2013, 402, 190-195.	5.0	44
46	Fractional-hydrolysis-driven formation of nonuniform dopant concentration catalyst nanoparticles of Cr/Ce x Zr 1â^' x O 2 and their catalysis in oxidation of NO. Chemical Engineering Journal, 2014, 236, 223-232.	6.6	44
47	Effects of Cr on the NO oxidation over the ceria–zirconia solid solution. RSC Advances, 2013, 3, 7009.	1.7	43
48	The formation of 3D spherical Cr-Ce mixed oxides with roughness surface and their enhanced low-temperature NO oxidation. Chemical Engineering Journal, 2018, 333, 414-422.	6.6	43
49	A Composite Catalyst Based on Perovskites for Overall Water Splitting in Alkaline Conditions. ChemElectroChem, 2019, 6, 1520-1524.	1.7	42
50	Haloid acid induced carbon nitride semiconductors for enhanced photocatalytic H2 evolution and reduction of CO2 under visible light. Carbon, 2018, 138, 465-474.	5.4	41
51	Efficient CO2 Utilization via a Hybrid Na-CO2 System Based on CO2 Dissolution. IScience, 2018, 9, 278-285.	1.9	40
52	Capture of carbon dioxide from flue gases by amine-functionalized TiO2 nanotubes. Applied Surface Science, 2013, 268, 124-128.	3.1	39
53	Treatment of carbon cloth anodes for improving power generation in a dual hamber microbial fuel cell. Journal of Chemical Technology and Biotechnology, 2013, 88, 623-628.	1.6	37
54	Solvent effects on formation of Cr-doped Ce0.2Zr0.8O2 synthesized with cinnamic acid and their catalysis in oxidation of NO. Chemical Engineering Journal, 2014, 246, 328-336.	6.6	36

#	Article	IF	CITATIONS
55	Electrochemical property of multi-layer anode supported solid oxide fuel cell fabricated through sequential tape-casting and co-firing. Journal of Materials Science and Technology, 2019, 35, 695-701.	5.6	36
56	Construction of Nano-Fe <sub>2</sub> O <sub>3</sub> -Decorated Flower-Like MoS <sub>2</sub> with Fe–S Bonds for Efficient Photoreduction of CO <sub>2</sub> under Visible-Light Irradiation. ACS Sustainable Chemistry and Engineering, 2020, 8, 12603-12611.	3.2	34
57	Evaluation of La0.4Ba0.6Fe0.8Zn0.2O3â~ì́rÂ+ÂSm0.2Ce0.8O1.9 as a potential cobalt-free composite cathode for intermediate temperature solid oxide fuel cells. Journal of Power Sources, 2015, 275, 808-814.	4.0	32
58	Synthesis and characterization of direct Z-scheme Bi2MoO6/ZnIn2S4 composite photocatalyst with enhanced photocatalytic oxidation of NO under visible light. Journal of Materials Science, 2017, 52, 11453-11466.	1.7	31
59	A high-performance, cobalt-free cathode for intermediate-temperature solid oxide fuel cells with excellent CO2 tolerance. Journal of Power Sources, 2016, 319, 178-184.	4.0	30
60	Stable, efficient and cost-competitive Ni-substituted Sr(Ti,Fe)O3 cathode for solid oxide fuel cell: Effect of A-site deficiency. Journal of Power Sources, 2020, 451, 227762.	4.0	30
61	Z-scheme Caln <sub>2</sub> S <sub>4</sub> /Ag <sub>3</sub> PO <sub>4</sub> nanocomposite with superior photocatalytic NO removal performance: fabrication, characterization and mechanistic study. New Journal of Chemistry, 2018, 42, 318-326.	1.4	29
62	Ni and Zn co-substituted Co(CO3)0.5OH self-assembled flowers array for asymmetric supercapacitors. Journal of Colloid and Interface Science, 2020, 573, 299-306.	5.0	28
63	Catalytic Oxidation of NO to NO2 Over Co–Ce–Zr Solid Solutions: Enhanced Performance of Ce–Zr Solid Solution by Co. Catalysis Letters, 2014, 144, 538-544.	1.4	27
64	New insights into intermediate-temperature solid oxide fuel cells with oxygen-ion conducting electrolyte act as a catalyst for NO decomposition. Applied Catalysis B: Environmental, 2014, 158-159, 418-425.	10.8	26
65	Advances and Perspectives for the Application of Perovskite Oxides in Supercapacitors. Energy & Fuels, 2021, 35, 17353-17371.	2.5	26
66	Ag and MOFs-derived hollow Co3O4 decorated in the 3D g-C3N4 for creating dual transferring channels of electrons and holes to boost CO2 photoreduction performance. Journal of Colloid and Interface Science, 2022, 609, 901-909.	5.0	26
67	Ferrous-based electrolyte for simultaneous NO absorption and electroreduction to NH3 using Au/rGO electrode. Journal of Hazardous Materials, 2022, 430, 128451.	6.5	26
68	Structural and electrochemical properties of B-site Mg-doped La0.7Sr0.3MnO3â~δ perovskite cathodes for intermediate temperature solid oxide fuel cells. Journal of Alloys and Compounds, 2016, 655, 99-105.	2.8	25
69	Solvent effects during the synthesis of Cr/Ce0.2Zr0.8O2 catalysts and their activities in NO oxidation. Chemical Engineering Journal, 2015, 270, 1-8.	6.6	24
70	The solvent-driven formation of multi-morphological Ag–CeO <sub>2</sub> plasmonic photocatalysts with enhanced visible-light photocatalytic reduction of CO <sub>2</sub> . RSC Advances, 2018, 8, 40731-40739.	1.7	23
71	A perovskite oxide with a tunable pore-size derived from a general salt-template strategy as a highly efficient electrocatalyst for the oxygen evolution reaction. Chemical Communications, 2019, 55, 2445-2448.	2.2	23
72	Electron-coupled enhanced interfacial interaction of Ce-MOF/Bi2MoO6 heterostructure for boosted photoreduction CO2. Journal of Environmental Chemical Engineering, 2022, 10, 107461.	3.3	23

#	Article	IF	CITATIONS
73	Performance of Y0.9Sr0.1Cr0.9Fe0.1O3â^î´as a sulfur-tolerant anode material for intermediate temperate solid oxide fuel cells. Journal of Power Sources, 2014, 250, 143-151.	4.0	22
74	Correlation of morphology with catalytic performance of CrO /Ce0.2Zr0.8O2 catalysts for NO oxidation via in-situ STEM. Chemical Engineering Journal, 2016, 288, 238-245.	6.6	21
75	Facile synthesis of hierarchical nickel–cobalt sulfide quadrangular microtubes and its application in hybrid supercapacitors. Journal of Materials Science: Materials in Electronics, 2017, 28, 18064-18074.	1.1	21
76	Facile fabrication of oxygen and carbon co-doped carbon nitride nanosheets for efficient visible light photocatalytic H <sub>2</sub> evolution and CO <sub>2</sub> reduction. Dalton Transactions, 2019, 48, 12070-12079.	1.6	21
77	Facile Dynamic Synthesis of Homodispersed Ni <sub>3</sub> S <sub>2</sub> Nanosheets as a Highâ€Efficient Bifunctional Electrocatalyst for Water Splitting. ChemCatChem, 2019, 11, 1320-1327.	1.8	21
78	Efficient and stable nanoporous functional composited electrocatalyst derived from Zn/Co-bimetallic zeolitic imidazolate frameworks for oxygen reduction reaction in alkaline media. Electrochimica Acta, 2019, 299, 610-617.	2.6	20
79	3D flower-like hierarchical Ag@nickel-cobalt hydroxide microsphere with enhanced electrochemical properties. Electronic Materials Letters, 2016, 12, 824-829.	1.0	19
80	A Controllable Dual Interface Engineering Concept for Rational Design of Efficient Bifunctional Electrocatalyst for Zinc–Air Batteries. Small, 2022, 18, e2105604.	5.2	18
81	Structure and redox properties of perovskite Y0.9Sr0.1Cr1â^'xFexO3â^'δ. Applied Surface Science, 2013, 268, 246-251.	3.1	17
82	Highly efficient simulated solar-light photocatalytic oxidation of gaseous NO with porous carbon nitride from copolymerization with thymine and mechanistic analysis. RSC Advances, 2016, 6, 101208-101215.	1.7	17
83	Spinel MnCo <sub>2</sub> O <sub>4</sub> /N,Sâ€doped Carbon Nanotubes as an Efficient Oxygen Reduction Reaction Electrocatalyst. ChemistrySelect, 2016, 1, 2159-2162.	0.7	16
84	Co(OH)2 particles decorated Ni3(NO3)1.6(CO3)0.2(OH)4 flower-like composite electrode for high-performance hybrid supercapacitors. Journal of Alloys and Compounds, 2020, 817, 152689.	2.8	16
85	CuO-decorated dual-phase TiO2 microspheres with enhanced activity for photocatalytic CO2 reduction in liquid–solid regime. Chemical Physics Letters, 2019, 725, 66-74.	1.2	14
86	A well-controlled three-dimensional tree-like core–shell structured electrode for flexible all-solid-state supercapacitors with favorable mechanical and electrochemical durability. Journal of Materials Chemistry A, 2021, 9, 16099-16107.	5.2	14
87	Mesoporous TiO2 as the support of tetraethylenepentamine for CO2 capture from simulated flue gas. RSC Advances, 2013, 3, 23785.	1.7	13
88	Facile preparation of porous carbon nitride for visible light photocatalytic reduction and oxidation applications. Journal of Materials Science, 2018, 53, 11315-11328.	1.7	13
89	Composites of Single/Double Perovskites as Cathodes for Solid Oxide Fuel Cells. Energy Technology, 2016, 4, 804-808.	1.8	11
90	A simple seed-mediated growth method for the synthesis of highly morphology controlled CrO x /Ce 0.2 Zr 0.8 O 2 catalysts and their enhanced NO oxidation. Chemical Engineering Journal, 2017, 317, 376-385.	6.6	11

#	Article	IF	CITATIONS
91	Interaction between electrode materials Sr2FeCo0.5Mo0.5O6â^' and hydrogen sulfide in symmetrical solid oxide fuel cells. International Journal of Hydrogen Energy, 2017, 42, 22266-22272.	3.8	11
92	Amorphous Core–Shell Nanoparticles as a Highly Effective and Stable Batteryâ€Type Electrode for Hybrid Supercapacitors. Advanced Materials Interfaces, 2019, 6, 1900858.	1.9	10
93	Turning the activity of Cr–Ce mixed oxide towards thermocatalytic NO oxidation and photocatalytic CO2 reduction via the formation of yolk shell structure hollow microspheres. Journal of Alloys and Compounds, 2020, 829, 154508.	2.8	10
94	Molecular-level proton acceptor boosts oxygen evolution catalysis to enable efficient industrial-scale water splitting. Green Energy and Environment, 2024, 9, 344-355.	4.7	10
95	Mesoporous Spinel Nanofibers and Nitrogenâ€doped Carbon Nanotubes as Highâ€Performance Electrocatalyst for Oxygen Reduction in Alkaline and Neutral Media. Energy Technology, 2017, 5, 283-292.	1.8	9
96	A Rational Design for Enhanced Catalytic Activity and Durability: Strongly Coupled N-Doped CrOx/Ce0.2Zr0.8O2 Nanoparticle Composites. ACS Applied Nano Materials, 2018, 1, 1150-1163.	2.4	9
97	Revealing Isolated Mâ^'N 3 C 1 Active Sites for Efficient Collaborative Oxygen Reduction Catalysis. Angewandte Chemie, 2020, 132, 23886-23891.	1.6	9
98	Validation and Electrochemical Characterization of LSCF Cathode Deposition on Metal Supported SOFC. Journal of the Electrochemical Society, 2017, 164, F1489-F1494.	1.3	7
99	Effect of an anode modified with nitrogenous compounds on the performance of a microbial fuel cell. Energy Sources, Part A: Recovery, Utilization and Environmental Effects, 2016, 38, 527-533.	1.2	6
100	Efficient Inhibition of N <sub>2</sub> O during NO Absorption Process Using a CuO and (NH <sub>4</sub> ) <sub>2</sub> SO <sub>3</sub> Mixed Solution. Industrial & Engineering Chemistry Research, 2018, 57, 13010-13018.	1.8	6
101	Construction of Z-scheme Photocatalyst Containing Znln2S4, Co3O4-Photodeposited BiVO4 (110) Facets and rGO Electron Mediator for Overall Water Splitting into H2 and O2. Catalysis Letters, 2021, 151, 2570-2582.	1.4	6
102	In situ fabrication of cobalt/nickel sulfides nanohybrid based on various sulfur sources as highly efficient bifunctional electrocatalysts for overall water splitting. Nano Select, 0, , .	1.9	6
103	Fabrication of core–shell C/MnO nanocomposite by liquid deposition for high performance lithium-ion batteries. Journal of Materials Science: Materials in Electronics, 2019, 30, 5978-5985.	1.1	5
104	Synthesis and performance of Sm0.9Sr0.1Cr0.5Fe0.5O3 as anode material for SOFCs running on H2S-containing fuel. Ionics, 2013, 19, 491-497.	1.2	4
105	Synthesis and characterization of Ca and Sr co-doped ceria electrolytes. Ionics, 2014, 20, 721-727.	1.2	4
106	Improvement of BaCe0.8Sm0.1Y0.1O3-δ-based IT-SOFC by optimizing spin-coated process of cathode and sintering temperature. Ionics, 2015, 21, 817-822.	1.2	4
107	Enhanced Light-driven CO2 Reduction on Metal-free Rich Terminal Oxygen-defects Carbon Nitride Nanosheets. Journal of Colloid and Interface Science, 2021, 608, 2505-2505.	5.0	4
108	La0.4Ba0.6Fe0.8Zn0.2O3â~ʾδas cathode in solid oxide fuel cells for simultaneous NO reduction and electricity generation. Environmental Technology (United Kingdom), 2014, 35, 925-930.	1.2	3

#	Article	IF	CITATIONS
109	Fabrication of Controllable N-Doped Ce0.2Zr0.8O2 via O–N–O Bond with Robust NO Oxidation and Durability at Low Temperature. Energy & Fuels, 2021, 35, 752-761.	2.5	2
110	Electrocatalysis: Porous Cobalt Phosphide Polyhedrons with Iron Doping as an Efficient Bifunctional Electrocatalyst (Small 40/2017). Small, 2017, 13, .	5.2	1
111	Sr(Ti,Fe)O <sub>3â^'δ </sub> Based Intermediate Temperature Solid Oxide Fuel Cell Anode with Self-precipitated (Ni,Fe) and Gd <sub>0.1</sub> Ce <sub>0.9</sub> O <sub>2â^´Î´ </sub> Nano Particles. Journal of the Electrochemical Society, 2020, 167, 164507.	1.3	1
112	Electrical and Electrochemical Performances Evaluation of LaNi <sub>0.6</sub> Fe <sub>0.4</sub> O <sub>3</sub> Cathode Contact and Current Collecting Layer in	1.3	1

SOFCs. Journal of the Electrochemical Society, 2022, 169, 044531.